J Intell Robot Syst (2007) 48:115–127
DOI 10.1007/s10846-006-9092-y

UNMANNED SYSTEMS PAPER

A Decomposed-model Predictive Functional Control Approach to Air-vehicle Pitch-angle Control

Igor Škrjanc

Received: 1 June 2006 / Accepted: 29 October 2006 /
Published online: 1 December 2006

Abstract The requirements for the pitch-angle control of an air vehicle are a very fast response with as few vibrations as possible. The vibrations can damage the equipment that is carried within the body of the vehicle. The main problem to deal with is the relatively fast and under damped dynamics of the vehicle and the slow actuators and sensors. We have solved the problem by using a predictive approach. The main idea of this approach is a process output prediction based on a decomposed process model. The decomposition enables the extension of the model-based approach to processes with integrative behavior such as in the case of a rocket's pitch-angle control. The proposed approach is not only useful in this case but it gives us a framework to design the control for a wide range of processes. We compared the predictive design methodology with the classical compensator control approach, known from aerospace system control. The advantage of the new approach is the reduced vibrations during the transient response.

Key words compensation · decomposition methods · modelling · predictive control · vibrations

1 Introduction

Air vehicles are very important in the life of modern people. Because of the lower safety requirements, like in other fields of robotics, the idea of an autonomous air vehicle has arisen. The aim of our project was to develop a control algorithm for the Unmanned Air Vehicle (UAV), which will be used to carry an Air-Turbo Ram Jet (ATR) engine during the engine tests. A helicopter will be used to carry the air vehicle into the air. At the required altitude, which is about 2,000 m above the

I. Škrjanc (✉)
Faculty of Electrical Engineering, University of Ljubljana, Tržaška 25,
1000 Ljubljana, Slovenia
e-mail: igor.skrjanc@fe.uni-lj.si

ground, the air vehicle will be dropped. After gaining enough speed the vehicle will be pulled-out to a cruising glide-path. During this cruise some measurements will be made, and then the vehicle will land using a parachute. The flight test can be divided into 8 stages: 1. drop from the helicopter, 2. nose dive to gain enough velocity, 3. pull-out, 4. glide cruise, 5. engine testing cruise, 6. deployment of the gliding parachute, 7. gliding and 8. final flare and landing.

Each stage of the experiment requires a special control attention from the control point of view because of the changing dynamics of the air vehicle. This means that each operating point, according to the velocity changes, changed weight of the air vehicle and/or the different flight regime, requires different control parameters. The nonlinear model of the air vehicle which is valid for all the regimes should be linearized at several operating points, to obtain a set of linear sub-models that are used to design the controllers for all the operating regimes. A gain-scheduling algorithm is then used to switch between the linear controllers. An introduction to qualitative feedback theory for flight control is given by [13], and a nonlinear approach to flight control design is given in [12].

Our main goal was to develop the algorithm to control the vehicle in the 4th stage. This means controlling the pitch-angle to follow the desired trajectory during the cruising phase of the experiment. The requirements for the pitch-angle control of a winged body are a very fast response with as few vibrations as possible. This is a difficult task because the very fast and under-damped dynamics of the body is combined with relatively slow actuators. There is another problem, of not knowing exactly the parameters of the process. The aerodynamic parameters are given in the range of $\pm 40\%$. They depend on the actual weather conditions, and a change of those parameters causes a serious control design problems, which should be robust across the whole range of parameter changes and should give an appropriate control performance. During this stage the velocity and the weight of the vehicle are relatively constant, because the testing engine is not jet started.

The previously applied control algorithm for the pitch-angle control of the UAV was realized by using a classical compensator. This led to an appropriate response in the case of nominal parameters, but for the wide range of aerodynamic parameter changes the responses were not satisfactory, especially because of high-frequency vibrations.

The idea is to implement a model-based predictive control strategy similar to those presented by [3, 9] and [10]. The basic idea given by [9] is given in the state space, what means the generalization of the design. In this paper it is extended to the processes with an integrative nature. In this case the model is decomposed into two parallel models and included into the design of the control law. This modification makes it possible to predict the future model output. The control algorithm is called a decomposed-model predictive functional control (DMPFC). The control law is then obtained using the basic principles of predictive control [5, 11]. The main advantage of our approach is the compact design in the state-space, which offers the framework to design the control for a wide range of different processes: integrative, phase non-minimal, with time-delay, as well as processes of higher order and multivariable processes. The problem of time-delay is solved in the same way as [3] and [4]. The issue of stability and strict robustness analysis can be discussed in a classical manner as given in [3] and are not discussed in this paper.

The paper is organized as follows: in Section 2 the modeling of the rocket dynamics is given, in Section 3 the decomposed-model predictive control algorithm is described and in Section 4 the simulation study is given, where the comparison with the previously used classical compensator is also presented.

2 The Dynamics of the Air Vehicle

The vehicle consists of a slender body, the wings and a four-fin tail stabilizer in an X shape. The rocket is modeled as a winged rigid body. Its shape and basic dimensions are given in Figure 1. The construction of the vehicle is symmetrical, which means the flight performance is the same when the vehicle is flying upside-down. In combination with a very thin airfoil of the wings and a very thin stabilizer that allows high speed, the vehicle has excellent manoeuvering capabilities.

In our case only the control of the longitudinal motion of the rocket will be treated, i.e., only the model $\frac{\Theta(s)}{\delta(s)}$ will be investigated, where Θ is the pitch angle and δ is the control fins' deflection angle. The diagram of the forces and torques is shown in Figure 2, where x and z represent the coordinates of the system, v is the airspeed, v_x and v_z are the airspeed components in the x and z coordinates, Θ is the pitch angle, Ω is the angular velocity, F_g is the gravitational force, F_L is the lift force, F_D is the drag force, F_x is the air-pressure force in the direction of the x axis, F_z is the air-pressure force in the direction of the z coordinate, M is the torque caused by the lift and drag, F_c is the control force, cp is the center of pressure, cg is the center of gravity, l_{cp} is the handle of the pressure center and l_{c} is the handle of the control force.

The motion of a rigid winged-body in all three dimensions can be represented by the Euler equations of motion [6, 8]. For a 2D problem the motion can be described with the following equations:

$$\begin{aligned} F_x - mg\sin\Theta &= m\left(\dot{v_x} + \Omega v_z\right) \\ F_z + mg\cos\Theta &= m\left(\dot{v_z} - \Omega v_x\right) \\ M &= I_y\dot{\Omega} \\ \Omega &= \dot{\Theta} \end{aligned} \tag{1}$$

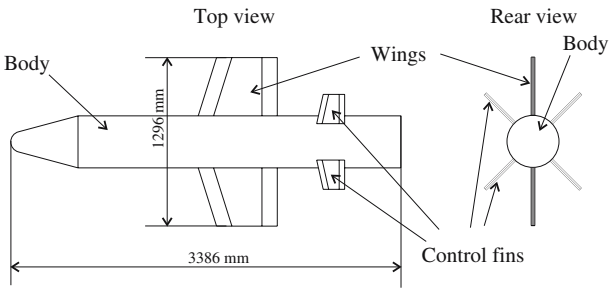

Figure 1 The shape and basic dimensions of the rocket.

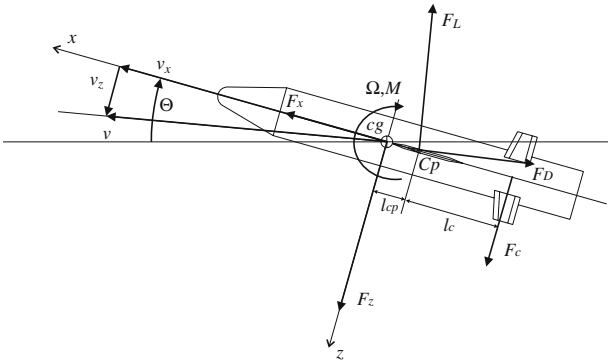

Figure 2 The diagram of forces and torques.

The airflow around the specific shape is difficult to describe using mathematical formulas, therefore the aerodynamic forces and moments are calculated using aerodynamic coefficients. For a winged body the following can be written:

$$\begin{aligned} F_L &= qSC_{L\alpha}\alpha \\ F_D &= qSC_D \\ q &= \frac{\rho v^2}{2} \\ \alpha &= \arctan\frac{v_z + \Omega l_{cp}}{v_x} \end{aligned} \tag{2}$$

where F_L and F_D are the lift and drag forces, S is the reference area, α is the angle of attack, and q is the dynamic pressure. The aerodynamic coefficients $C_{L\alpha}$ and C_D denote the lift coefficient and the drag coefficient, respectively. They are usually measured and given as a look-up table. Both coefficients vary in the range of about ±40%. This means that the implied control needs to have great robustness. The x and z components of the body force for the geometry of Figure 2 can be written as follows:

$$\begin{aligned} F_{XB} &= -F_D\cos\alpha + F_L\sin\alpha \\ F_{ZB} &= -F_L\cos\alpha - F_D\sin\alpha \end{aligned} \tag{3}$$

The lift and drag forces also cause some torque. This can be calculated by multiplying these forces by the distance between the center of gravity and the center of pressure. This distance depends on the angle of attack α. To calculate the torque of the body the following equation is used:

$$M_B = qSlC_{M\alpha}\alpha \tag{4}$$

where l is the reference length and $C_{M\alpha}$ is another coefficient that stands for:

$$C_{M\alpha} = C_{L\alpha}\frac{l_{cp}}{l} \tag{5}$$

and is also usually given in a look-up table. A deflection of the control surface by an angle δ results in the control force F_C:

$$F_C = qSC_{L\delta}\delta \tag{6}$$

The shape of the rocket is rather unusual: four tail fins are set in the shape of the letter X, as shown in Figure 1. The aileron, elevator and rudder (roll, pitch and yaw) effects are given by a combination of the tail fins' deflections. The deflection of the X-shaped fins has a coupling effect on the vehicle's dynamics, on the roll, pitch and yaw angle. The effect of the coupling is compensated by a recalculation or a combination of the tail fins' deflections, which is based on the geometry and the position of the control fins.

The control torque is obtained by multiplying the control force by the distance to the axis of rotation (the center of gravity). When the control surfaces work as an elevator the x and z components of the control force (F_{XC} and F_{ZC}) and the control torque (M_C) are:

$$\begin{aligned} F_{XC} &= n_e F_C \sin\alpha \\ F_{ZC} &= n_e F_C \cos\alpha \\ M_C &= F_{ZC} l_c \end{aligned} \tag{7}$$

with $n_e = 2\sqrt{2}$.

The common forces and torques of the body and the control surfaces are:

$$\begin{aligned} F_X &= F_{XB} + F_{XC} \\ F_Z &= F_{YB} + F_{ZC} \\ M &= M_B + M_C \end{aligned} \tag{8}$$

The nonlinear model of the rocket dynamics is described in Eq. 8. For control purposes, this model can be linearized to obtain a simpler linear model.

The model was linearized around the following stationary state: $v_x = 75$ m s^{-1}, $v_z = 0$, $\alpha = 0$, $\Omega = 0$ and $\Theta = 0$, and we obtained the following transfer function:

$$G_{rb}(s) = \frac{\Omega(s)}{\delta_a(s)} = \frac{n_e (b_1 s + b_0)}{\left(s^2 + a_1 s + a_0\right)} \tag{9}$$

where $G_{rb}(s)$ stands for the rocket-body transfer function between the pitch-angle velocity Ω and the angle of the deflection fins δ_a. The parameters a_1, a_0, b_1 and b_0 stand for:

$$\begin{aligned} a_1 &= \frac{qSC_{L\alpha}}{mv_x} + \frac{qSC_{M\alpha} l l_{cp}}{I_y v_x} \\ a_0 &= -\frac{qSC_{M\alpha} l}{I_y} \\ b_1 &= \frac{qSC_{L\alpha} l_c}{I_y} \\ b_0 &= \frac{q^2 S^2 C_{L\delta}}{mv_x I_y} \left(C_{L\alpha} l_c + C_{M\alpha} l\right) \end{aligned} \tag{10}$$

with the following values of the parameters at the point of linearization: $l = 3.386$ m, $m = 260$ kg, $S = 0.12566$ m^2, $I_y = 253.1$ kg m^2, $C_{M\alpha} = -0.6393$, $C_{L\alpha} = 23.5$, $C_{L\delta} = 3.0197$, $l_c = -0.8285$ m, $l_{cp} = -0.0921$ m.

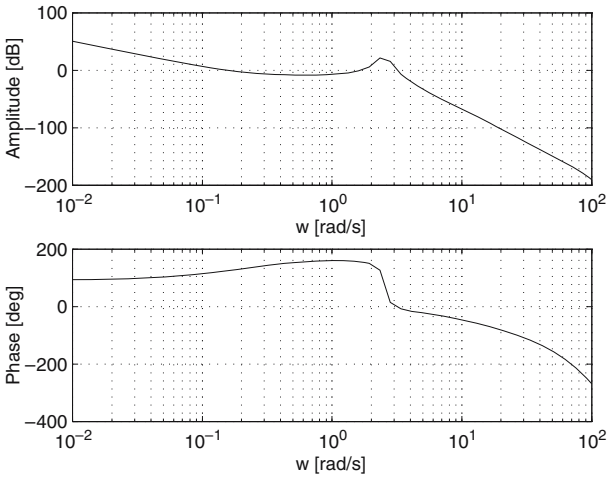

Figure 3 The frequency response of the rocket system.

Another problem is caused by the constraints of the deflection fins in the range of -0.05 rad $\leq \delta \leq 0.05$ rad and the dynamics of the angular velocity sensor. The transfer functions of both are as follows:

$$G_a = \frac{\delta_a(s)}{\delta(s)} = \frac{\omega_1^2}{s^2 + 2\zeta_1\omega_1 s + \omega_1^2} \frac{\tau_{a_1} s + 1}{\tau_{a_2} s + 1}$$

$$G_s = \frac{\Omega_s(s)}{\Omega(s)} = \frac{\omega_2^2}{s^2 + 2\zeta_2\omega_2 s + \omega_2^2} \frac{-\tau s + 1}{\tau s + 1} \tag{11}$$

where δ_a is an input to the actuator, Ω_s is the output from the angular velocity sensor and where $\omega_1 = 28\pi$ rad s^{-1}, $\zeta_1 = 0.5$, $\frac{1}{\tau_{a_1}} = 40\pi$ s^{-1}, $\frac{1}{\tau_{a_2}} = 5\pi$ s^{-1}, and $\omega_2 = 54\pi$ rad s^{-1}, $\zeta_2 = 0.5$, $\tau = 0.0085$ s.

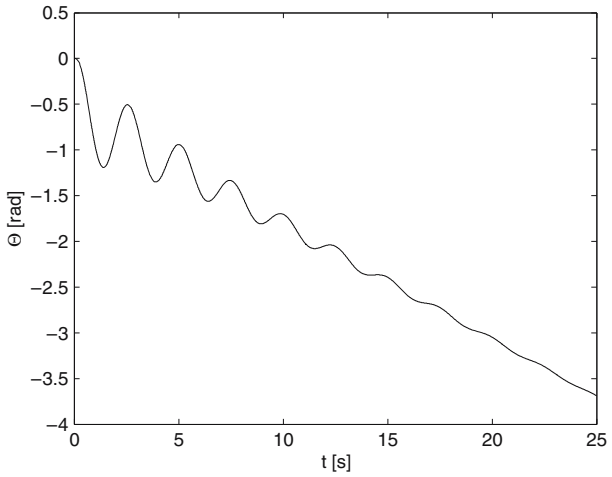

Figure 4 The step response of the rocket system.

Taking into account the rocket dynamics, the actuator and the sensor, the dynamics of the whole process is as follows:

$$G_r(s) = \frac{\Omega_s(s)}{\delta(s)} = G_a(s)G_{rb}(s)G_s(s)e^{-sT_d} \tag{12}$$

where T_d stands for the time-delay that is due to the computational time and is equal to $T_d = 0.015$ s.

The frequency response of the whole process is shown in Figure 3. The small resonance frequency peak of the rocket system appears at a frequency of 2.1 rad/s. Figure 4 shows the step response of the open-loop system, where the high-frequency vibrations are clear.

3 Decomposed-model Predictive Control Law

The model-based predictive formulation for the control of open-loop unstable processes is frequently used as an optimization control problem [7]. In the case of fast and open-loop unstable processes this approach cannot be implemented. The realization requirements demand a computation algorithm that can be calculated very quickly so as not to enlarge the computational time delay. This means that the control algorithm should be given in an analytical way.

In this section the main idea behind the decomposed-model predictive control will be given. It is given in the discrete-time domain, which is the most natural for predictive techniques. Let the process model be the following:

$$\begin{aligned} x_m(k+1) &= \mathbf{A}_m x_m(k) + \mathbf{B}_m u(k) \\ y_m(k) &= \mathbf{C}_m x_m(k) \end{aligned} \tag{13}$$

where $\mathbf{A}_m, \mathbf{B}_m$ and $\mathbf{C}_m$ are the time-discrete state-space matrices of the process model, without taking into account the process delay.

The main idea of the predictive algorithm [11] is to determine the future control action so that the predicted output value coincides with the reference trajectory. The point where the reference and output signal coincide is called the coincidence horizon and is denoted by H. The prediction is calculated by assuming a constant future control variable ($u(k) = u(k+1) = \ldots = u(k+H-1)$), i.e., the mean level control. With this assumption the H-step ahead prediction of the model output at the time instant k can be easily obtained, as follows:

$$y_m(k+H|k) = \mathbf{C}_m \left(\mathbf{A}_m^H \mathbf{x}_m(k) + \mathbf{K}u(k)\right) \tag{14}$$

with $\mathbf{K} = \left(\mathbf{A}_m^H - \mathbf{I}\right)(\mathbf{A}_m - \mathbf{I})^{-1}\mathbf{B}_m$. When the system matrix $\mathbf{A}_m$ is Hurwitz, then the predictive control law can be calculated using the prediction in Eq. 14. In the case of integrative behavior the system matrix $\mathbf{A}_m$ is not Hurwitz [1] and the proposed prediction cannot be applied. In this case the process model transfer function should be decomposed in the following way:

$$G_m(z) = G_{m_p}(z) + G_{m_i}(z) \tag{15}$$

where $G_{m_p}(z)$ and $G_{m_i}(z)$ stand for the proportional and pure integrative parts.

The state-space equivalent of the transfer function $G_{m_p}(z)$ is described by the matrices $\mathbf{A}_{m_1}, \mathbf{B}_{m_1}$ and $\mathbf{C}_{m_1}$ and the state-space equivalent $\mathbf{A}_{m_2}, \mathbf{B}_{m_2}$ and $\mathbf{C}_{m_2}$ for the

transfer function $G_{m_i}(z)$. The prediction of the process model output is calculated as the sum of both predictions

$$\begin{aligned} y_{m_1}(k+H) &= \mathbf{C}_{m_1}\left(\mathbf{A}_{m_1}^H \mathbf{x}_{m_1}(k) + \mathbf{K}_m u(k)\right) \\ y_{m_2}(k+H) &= \mathbf{C}_{m_2}\left(\mathbf{x}_{m_2}(k) + H\mathbf{B}_{m_2}\right) u(k) \end{aligned} \tag{16}$$

with $\mathbf{K}_m = \left(\mathbf{A}_{m_1}^H - \mathbf{I}\right)\left(\mathbf{A}_{m_1} - \mathbf{I}\right)^{-1}\mathbf{B}_{m_1}$ and is given as follows

$$y_m(k+H) = y_{m_1}(k+H) + y_{m_2}(k+H) \tag{17}$$

The behavior of the closed-loop system in the case of the proposed predictive control technique is defined by the reference trajectory given by the reference-model transfer function. The reference-model trajectory is given implicitly by the exponential factor, which describes how the control error should behave in the future. Through this exponential factor, which is analogous to the time constant of the reference model, we will predict the control error for the H-step ahead, at the so-called coincidence horizon, as follows:

$$w(k+H) - y_p(k+H) = a_r^H \cdot \left(w(k) - y_p(k)\right) \tag{18}$$

where $w(k)$ and $y_p(k)$ are the current reference signal and output signal of the process and a_r denotes the pole of the reference model. Assuming the equivalence of the predicted reference model trajectory and the estimated process output at the coincidence horizon and the constant reference signal in the future ($w(k) = w(k+1) = \ldots = w(k+H)$), the reference trajectory or the desired dynamics of the process output is given implicitly as follows:

$$y_p(k+H) = w(k) - a_r^H \cdot \left(w(k) - y_p(k)\right) \tag{19}$$

where a_r implicitly describes the reference-model trajectory.

The main goal of the proposed algorithm is to find the control law that enables the reference-trajectory tracking of the controlled signal. In other words, $u(k)$ has to be found to fulfill Eq. 19. The process output value can be estimated as

$$\hat{y}_p(k+H) = y_p(k) + y_m(k+H) - y_m(k) \tag{20}$$

It is obtained with the assumption that the plant output will change by the same amount as its model in the same interval of time.

Combining Eqs. 19, 20 and the prediction of the model output given in Eq. 17, the following is obtained:

$$\begin{aligned} u(k) &= g_0^{-1}\left(\left(1 - a_r^H\right)\left(w(k) - y_p(k)\right) + \mathbf{F}\mathbf{x}_{m_1}(k)\right) \\ \mathbf{F} &= \mathbf{C}_{m_1}\left(\mathbf{I} - \mathbf{A}_{m_1}^H\right) \end{aligned} \tag{21}$$

where g_0 stands for:

$$g_0 = \mathbf{C}_{m_1}\left(\mathbf{A}_{m_1}^H - \mathbf{I}\right)\left(\mathbf{A}_{m_1} - \mathbf{I}\right)^{-1}\mathbf{B}_{m_1} + H\mathbf{C}_{m_2}\mathbf{B}_{m_2} \tag{22}$$

The control law in Eq. 21 is valid for the process without time-delay. When we are dealing with a time-delayed process then the undelayed process output should be estimated. The estimation of the undelayed process output $\hat{y}_p(k)$ can be made on the

basis of the current process output and the delayed and undelayed process model outputs, as follows:

$$\hat{y}_p(k) = y_p(k) - y_m(k-d) + y_m(k) \tag{23}$$

where $y_m(k-d)$ stands for the d-samples delayed process model, where $d = round(\frac{T_d}{T_s})$. The control law of the DMPFC in the case of a time-delayed process is given as:

$$\begin{aligned} u(k) &= K_d\left(w(k) - \hat{y}_p(k)\right) + K_{x_{m_1}}\mathbf{x}_{m_1}(k) \\ K_d &= g_0^{-1}\left(1 - a_r^H\right) \\ K_{x_{m_1}} &= g_0^{-1}\mathbf{C}_{m_1}\left(\mathbf{I} - \mathbf{A}_{m_1}^H\right) \end{aligned} \tag{24}$$

Note that the DMPFC control law is realizable if the gain g_0 is non-zero. This is true if $H \geq \rho$, where ρ is the relative order of the system.

3.1 Constrained Control Law

When we deal with the process where the control signal is constrained by value the problem is solved as follows:

$$u_c(k) = \begin{cases} u_{min}, & u(k) < u_{min} \\ u(k), & u_{min} \leq u(k) \leq u_{max} \\ u_{max}, & u(k) > u_{max} \end{cases} \tag{25}$$

where u_{min} and u_{max} stand for the minimal and the maximal value of the control signal. The constrained control signal implicitly influence on the process-model states because of the internal model approach. This means that the constrained control signal which is the input to the real process is also input to the internal process model to obtain the states $\mathbf{x}_{m_1}$ of the process model, which are need to calculate the control law in Eq. 24.

4 Simulation Study

The proposed DMPFC approach was tested by simulation and compared with the simple compensator that is designed to have the same settling time as the previously designed DMPFC. The simulation study was performed for the 4th stage of the launch on the nonlinear model of the air vehicle. During this stage of the launch the velocity and the mass of the air vehicle is assumed to be constant.

To design the pitch-angle control of the rocket, we have to take into account the dynamics of the whole process, together with the actuators and sensors. The transfer function between the control signal δ and the measured pitch angle Θ_s is given as

$$G_c(s) = \frac{\Theta_s(s)}{\delta(s)} = \frac{1}{s}G_r(s) \tag{26}$$

The transfer function $G_c(s)$ is then decomposed into the parallel decomposition. In general this means that the systems with transfer function $\frac{B(s)}{sA(s)}$, where $A(s) \neq 0$ for $s = 0$, should be decomposed into

$$\frac{B(s)}{sA(s)} = \frac{Q(s)}{A(s)} + \frac{K}{s} = G_{m_p}(s) + G_{m_i}(s) \tag{27}$$

where $A(s) = a_n s^n + a_{n-1}s^{n-1} + ... + a_0$ and $B(s) = b_n s^n + b_{n-1}s^{n-1} + ... + b_0$.

The solution of the Diofantine equation in Eq. 27 is the following:

$$\begin{aligned} Ka_0 &= b_0 \\ q_i + Ka_{i+1} &= b_{i+1}, \quad i = 0, ..., n-1 \end{aligned} \tag{28}$$

where $Q(s) = q_{n-1}s^{n-1} + q_{n-2}s^{n-2} + ... + q_0$.

After the decomposition of the continuous transfer function into the parallel form, both transfer functions $G_{m_p}(s)$ and $G_{m_i}(s)$ are transformed into the discrete-time state-space presentation. This makes it possible to calculate the DMPFC parameters. To obtain a suitable performance and the appropriate robustness of the control in this case, the DMPFC was tuned to have the following parameters: $T_r = 7$ s and $H = 5$. The algorithm was implemented using a sampling time of $T_s = 0.01$ s. The tuning parameters result in the control parameters $K_d = -0.9297$ and $K_{x_{m_1}} = [-0.3959,\ 0.3967]$.

The DMPFC control algorithm was compared to the previously applied control algorithm, which was realized by using a classical compensator. Such compensators are very frequently used in aerospace control systems, because of their simplicity, robustness and good performance [2].

The control law of the compensator is the following:

$$\delta(s) = K_p\left(\Theta_r(s) - \Theta_s(s)\right) - K_r \cdot G_f(s)\Omega_s(s) \tag{29}$$

where $\Theta_r(s)$ stands for the Laplace transform of the reference signal, $K_p = -2.2383$, $K_r = -0.7967$ and $G_f(s)$ stands for the filter of the pitch-angle velocity

$$G_f(s) = \frac{\omega_f^2}{s^2 + 2\zeta_f\omega_f s + \omega_s^2} \tag{30}$$

where $\omega_f = 20\pi$ rad s^{-1} and $\zeta_f = 0.8$. The parameters of the proposed compensator were obtained with an optimization where the criterion of the settling time was used.

The control results and the comparison of both control algorithms for the nominal values of the system parameters are shown in Figure 5.

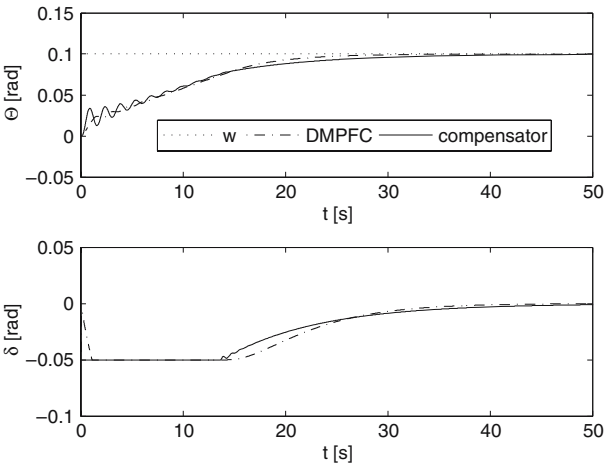

Figure 5 The comparison between simple compensation control and DMPFC control.

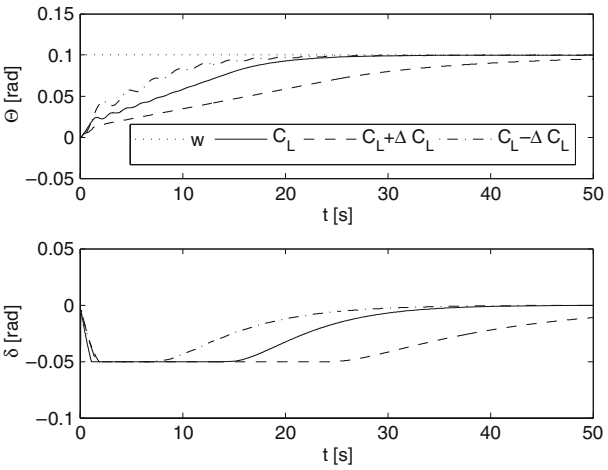

Figure 6 The DMPFC control for different values of system parameters.

Figure 5 shows that both responses have approximately the same settling time, but very different transient behavior. The compensator approach shows a response with large vibrations in the transient, which in the case of the DMPFC are almost absent. Both control algorithms do not reject the input disturbance, but this is actually not necessary in the case of attitude control.

The robustness in our case is of great importance because the aerodynamic coefficients $C_{L\alpha}$ and $C_{L\delta}$ vary in the range of about $\pm 40\%$ from the nominal value ($C_{L\alpha} = C^n_{L\alpha}(1 \pm 0.4)$, $C_{L\delta} = C^n_{L\delta}(1 \pm 0.4)$), where $C^n_{L\alpha}$ and $C^n_{L\delta}$ stand for the nominal values. We have simulated the closed-loop behavior where the controller was designed for the nominal values of the parameters and the process parameters have changed in the proposed range. All three responses, for the nominal case of the process parameters, for the positive deviation of the parameters and for the negative deviation of the parameters, were investigated.

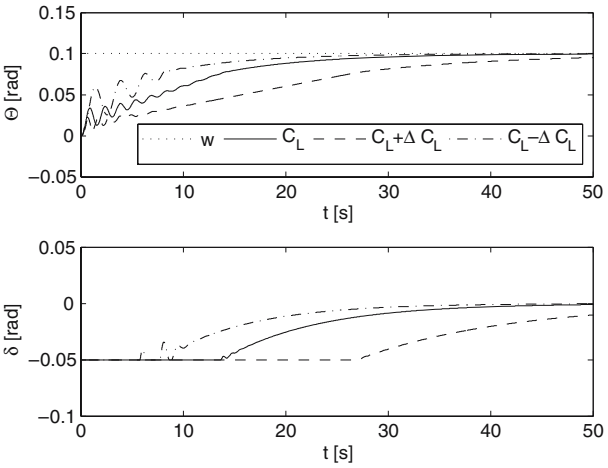

Figure 7 The compensation control for different values of system parameters.

In Figure 6 we show the influence of the system parameter changes on the performance of the DMPFC control algorithm. It is clear that the closed-loop responses in the case of process-parameter mismatch satisfy the normal performance requirements.

The same simulation was also performed for the compensator case, as shown in Figure 7. The obtained results show that the control is less robust than in the case of the DMPFC, in spite of the fact that the nominal response of the DMPFC is slightly faster than in the compensator case.

5 Conclusion

Decomposed-model predictive control was implemented to control the pitch angle of a rocket. The proposed control approach is not limited to this type of process, it can also be implemented in a wide range of different processes. The main advantage of the proposed approach is the very simple design, which results in better performance as proposed before. To show the potential use of the proposed approach, we made a comparison with classical compensator control, which is a known approach for controlling the pitch angle of the rocket. The robust performance of the proposed approach was also examined using a simulation, and it was shown that the proposed approach offers more robustness and better performance than the classical approach, especially in terms of the amount of vibration during the transient response.

Acknowledgements The work was done in the frame of a bilateral project between the Japan Society for the Promotion of Science, ISAS – Institute of Space and Astronautical Science, and the Ministry of Education, Science and Sport of the Republic of Slovenia, Faculty of Electrical Engineering, Ljubljana: Attitude Control of the Winged Test Vehicle. The author would like to thank to both institutions for their support.

References

1. Braatz, R.D.: Internal model control. In: Control Handbook, pp. 215–224. CRC Press, Butterworths, UK (1996)
2. Buschek, H., Calise, A.J.: Aerospace control system design with robust fixed order compensators. Aerosp. Sci. Technol. **1**(6), 391–404 (1997)
3. Kaya, I.: Imc based automatic tuning method for pid controllers in a smith predictor configuration. Comput. Chem. Eng. **28**, 281–290 (2004)
4. Lee, Y., Lee, J., Park, S.: Pid controller tuning for integrating and unstable processes with time delay. Chem. Eng. Sci. **55**, 3481–3493 (2000)
5. Lepetić, M., Škrjanc, I., Chiacchiarini, H.G., Matko, D.: Predictive functional control based on fuzzy model: comparison with linear predictive functional control and pid control. J. Intell. Robot. Syst. **36**(4), 467–480 (2003)
6. Moormann, D., Mosterman, P.J., Looye, G.: Object oriented computational model building of aircraft flight dynamics snd systems. Aerosp. Sci. Technol. **3**(3), 115–126 (1999)
7. Nagrath, D., Prasad, V., Bequette, B.W.: A model predictive formulation for open-loop unstable cascade systems. Chem. Eng. Sci. **57**, 365–378 (2002)
8. Pradeep, S.: Derivation of perturbed equations of motion of aircraft. Aircr. Des. **1**(4), 205–216 (1998)
9. Richalet, J.: Industrial application of model based predictive control. Automatica **29**(5), 1251–1274 (1993)
10. Tan, W., Marquez, H.J., Chen, T.: Imc design for unstable processes with time delays. J. Process Control **13**, 203–213 (2003)

11. Škrjanc, I., Matko, D.: Predictive functional control based on fuzzy model for heat-exchanger pilot plant. IEEE Trans. Fuzzy Syst. **8**(6), 705–712 (2000)
12. Wang, J., Sundararajan, N.: A nonlinear flight controller design for aircraft. Control Eng. Pract. **3**(6), 813–826 (1995)
13. Wu, S.F., Grimble, M.J., Breslin, S.G.: Introduction to quantitative feedback theory for lateral robust flight control systems design. Control Eng. Pract. **6**(7), 805–828 (1998)